Original Article

Synthesis and characterization of magnetic nanoparticle-incorporated nanohydroxyapatite and calcium and phosphate ion clusters for biomimetic remineralization of enamel and dentin

Ram Chowdary Basam, Nagesh Bolla, Sayesh Vemuri, Roopadevi Garlapati, Ankineedu Babu Dasari[1], Lahari B[2]

Departments of Conservative Dentistry and Endodontics, [2]Clinical Research, Sibar Institute of Dental Sciences, Guntur, Andhra Pradesh, India, [1]Department of Operative Dentistry, Meharry Medical College School of Dental Sciences, Nashville, Tennessee, USA

Abstract

Aim: The present study aimed to synthesize and characterize magnetic nanoparticle incorporated nanohydroxyapatite (MNHAP), calcium and phosphate ion clusters (CPICs), and their combination with MNHAP.

Materials and Methods: Nanohydroxyapatite (NHAP), magnetite (Fe_3O_4), and magnetic nanoparticle-incorporated nanohydroxyapatite (MNHAP) were synthesized using wet precipitation method, co-precipitation method, and ultrasonic-assisted mechanical stirring methods, respectively. CPIC was synthesized by centrifugation method. Their characterizations were analyzed through X-ray diffraction (XRD) crystallography, Fourier-transform infrared spectroscopy (FTIR), vibrating sample magnetometer (VSM), and high-resolution transmission electron microscopy. The biocompatibility of MNHAP was assessed through the 3-(4,5-dimethylthiazol-2-yl)-2,5-diphenyltetrazolium bromide assay.

Results: XRD substantiated the presence of diffraction peaks, indicating crystallinity in all synthesized samples. Functional groups in NHAP and MNHAP were confirmed through FTIR analysis. VSM analysis demonstrated superparamagnetic behavior in both MNHAP and Fe_3O_4. Transmission electron microscope images unveiled the needle-like crystals for NHAP, rod-shaped crystals for MNHAP, and polyhedral shapes for CPIC combined with MNHAP (CPIC + MNHAP). MNHAP exhibited biocompatibility up to 200 μg.

Conclusion: Based on the findings of this study, MNHAP and CPIC + MNHAP may be suitable for the repair of initial caries lesions.

Keywords: Calcium and phosphate ion clusters; magnetite; MNHAP; nanohydroxyapatite; remineralization

INTRODUCTION

Nanotechnology is constantly expanding in the domain of the synthesis of nanoparticles through different methods. It implies producing, handling, and operating materials at the atomic and nanoscale level, typically between 1 and 100 nm.[1] Changes in the configuration of the substrate from the macro to the nanoscale result in surpassing physical and chemical properties, simulating the nanostructure of the original tissue.[2,3] The compositional characteristics of nanoscale materials differ from the bulk materials. The differences in their properties arise from their increased surface area-to-volume ratio, leading to a higher number of surface atoms,[4] and enhanced electromagnetic interactions.[5]

Address for correspondence:
Dr. Ram Chowdary Basam,
Department of Conservative Dentistry and Endodontics,
Sibar Institute of Dental Sciences, Takkellapadu,
Andhra Pradesh, India.
E-mail: rambasamc@gmail.com

Date of submission : 30.09.2024
Review completed : 21.10.2024
Date of acceptance : 04.11.2024
Published : 10.12.2024

Access this article online

Quick Response Code:

Website: https://journals.lww.com/jcde

DOI: 10.4103/JCDE.JCDE_707_24

How to cite this article: Basam RC, Bolla N, Vemuri S, Garlapati R, Dasari AB, Lahari B. Synthesis and characterization of magnetic nanoparticle-incorporated nanohydroxyapatite and calcium and phosphate ion clusters for biomimetic remineralization of enamel and dentin. J Conserv Dent Endod 2024;27:1294-9.

Hydroxyapatite ($Ca_{10}(PO_4)_6(OH)_6$) is the most enduring form of calcium phosphate which contains calcium and phosphate and is similar to hydroxyapatite in the bone. It is the major inorganic constituent in the enamel and dentin, comprising 97% and 75% by weight, respectively. Prismatic enamel hydroxyapatite crystals range from 3 to 5 µm in diameter. Unlike hydroxyapatite crystals in the bone, those in the enamel, lack regenerative cells to remineralize the lost enamel, after demineralization.[6,7]

The quantitative Ca/P molar ratio in hydroxyapatite is about 1.6–1.7.[6] The nanohydroxyapatite crystals are available with a size ranging between 50 and 1000 nm and are synthesized using "top-down" and "bottom-up" methods.[8] Various remineralizing strategies, such as NHAP, bioactive glass, and casein phosphopeptide-amorphous calcium phosphate, have been explored in recent years to manage dental caries.[9-11] Nanohydroxyapatite (NHAP), with its smaller size and increased surface area, binds to the proteins, remineralizing the eroded areas and depressions created during demineralization. It can also penetrate the dentinal tubules, sealing them and thereby preventing exposure to external stimuli. NHAP has a high affinity for the hydroxyapatite crystals in enamel and dentin, decelerating supplementary demineralization caused by erosion.[6]

Magnetic nanoparticles have been used broadly in various scientific fields, including physics, chemistry, medicine, and dentistry. Magnetite (Fe_3O_4) nanoparticles with their superparamagnetic behavior and biocompatibility are extensively applied in the medical field to treat hyperthermia.[12] In addition, incorporating them into dentin-bonding agents has been shown to increase bond strength and remineralize dentin.[13] Calcium phosphate ion clusters (CPICs) through the controllable removal of ethanol and triethylamine showed the formation of well-oriented apatite crystals. They increased the hardness of enamel samples by their conversion to amorphous calcium phosphate and hydroxyapatite within 15 min and 48 h, respectively.[14]

Incorporating Fe_3O_4 into NHAP (MNHAP) and using CPIC in combination with MNHAP (CPIC + MNHAP) might enhance the remineralization of demineralized enamel and dentin by applying an external magnetic field. The present study aims to synthesize and characterize the nanohydroxyapatite NHAP, MNHAP, CPIC, and CPIC + MNHAP.

MATERIALS AND METHODS

Synthesis of NHAP

In summary, to synthesize pure hydroxyapatite by wet precipitation method, a solution of 0.1M $Ca(NO_3)_2.4H_2O$ (150 ml) was stirred continuously at room temperature, whereas 0.06M $(NH_4)2HPO_4$ (150 ml) was added dropwise. The pH was maintained at 10 with NH_4OH solution. After stirring for 30 min, the precipitate was allowed to age for 24 h, then centrifuged at 5000 rpm, and washed several times with water to remove any by-products. Finally, the product was freeze-dried at −50°C.[15]

Synthesis of Fe_3O_4 magnetic nanoparticle

The preparation of Fe_3O_4 nanoparticles was carried out using the co-precipitation method, which has been previously described. A solution containing 1 mol/L of $FeSO_4.7H_2O$ and 2 mol/L of $FeCl_3.6H_2O$ in a molar ratio of 1:2 was prepared. Next, 30 mL of 12 mol/L NH_4OH was added incrementally, drop by drop to the solution while mixing continuously till the formation of a black precipitate. The resulting black precipitate was aged for 24 h, then flushed three times with double distilled water and desiccated overnight at 100°C.[16]

Synthesis of Fe_3O_4 incorporated nanohydroxyapatite (MNHAP)

The magnetic nanoparticle, weighing 100 mg, was mixed with a solution of 0.1 M $Ca(NO_3)_2.4H_2O$ (150 ml). Dropwise addition of 0.06 M $(NH_4)2HPO_4$ solution followed, while the mixture was consigned to ultrasonication-facilitated mechanical stirring for an hour, and the pH was sustained at 10 by incorporating NH_4OH solution. After stirring for 30 min, the precipitate was allowed to age for 24 h, centrifuged at 5000 rpm, and cleansed multiple times with double-distilled water. The final product was then freeze-dried.[17]

Synthesis of calcium phosphate ion cluster solution

First, 0.20 g of $CaCl_2 \cdot 2H_2O$ and 3.8 ml of triethylamine were mixed with 80 ml of ethanol to prepare solution A. This solution was then subjected to ultrasonication for 5 min. Second, 70 µl of H_3PO_4 was combined with 20 ml of ethanol to formulate solution B, which was stirred intensely. Solution B was then combined with solution A with mild stirring. Consequently, CPICs were formulated in the suspension at a concentration of 2 mg/ml. The CPICs were in a gel-like state and were collected through centrifugation at 30,427 relative centrifugal force. The CPICs were then washed twice with ethanol.[14]

Preparation of calcium and phosphate ion clusters + MNHAP

1 mg/ml of MNHAP is added to CPIC with ethanol.

Characterizations

Powder X-ray diffraction crystallography

To obtain the structure and phase of the synthesized particles, a Rigaku MiniFlex-II powder X-ray diffractometer was used at 2 θ range of 20°–65°, using CuKa radiation with a wavelength of 1.5406 Å.[17]

Vibrating sample magnetometer analysis for Fe_3O_4 and MNHAP

The magnetic characteristics of synthesized magnetic nanoparticles (MNP) magnetite (Fe_3O_4) and magnetic nanoparticles encased with nanohydroxyapatite (MNHAP) were assessed using a Physical Property Measurement System (PPMS Evercool-2, Quantum Design, Inc.) with a vibrating sample magnetometer (VSM). To ascertain both the coercivity (HC) and saturation magnetization (MS) of the samples, M-H plots were documented at temperatures of 5K and 300K, with the maximum magnetic field range of 9 Tesla.[17]

Cytotoxicity of MNHAP

3-(4,5-dimethylthiazol-2-yl)-2,5-diphenyltetrazolium bromide assay (MTT assay) with gingival fibroblast cells was used to analyze the synthesized MNHAP. 1000 µg/mL of MNHAP was immersed in Dulbecco's Modified Eagle Medium F12 (F12 DMEM) without fetal bovine serum. The different concentrations of 50, 100, 200, 300, 400, 500, and 600 µg/mL media with MNHAP were obtained after 24 h and 48 h of submersion and dealt with gingival fibroblast cells to assess the compatibility. Each well containing 50,000 cells procured 500 µL of test samples submerged in media. 10 µL/100 mL of MTT reagent (5 mg/mL stock) was incorporated after 24 h to the cultured cells and incubated for 4 h at 37°C to allow formazan dye to develop. The medium is substituted for dimethyl sulfoxide (200 µL) and lasts 10 min. ELISA plate reader was used to measure the A590 after transferring the product to a 96-well ELISA plate. The percentage of cell viability was calculated using the equation. Cell viability (%) = $(OD_{Sample\ C}/OD_{Control}) \times 100$.[18]

Fourier transform Infrared spectroscopy

The analysis of functional groups present in the synthesized NHAP and MNHAP was performed using the KBr pellet technique in Bruker alpha II Fourier-transform infrared spectroscopy (FTIR) spectrometer with spectral region of 4000–400 cm^{-1} and 4 cm^{-1} resolution.[17]

High-resolution transmission electron microscopy examination

To evaluate the morphology of the synthesized NHAP, MNHAP, and CPIC + MNHAP. They are visualized under high-resolution transmission electron microscopy Jeol/JEM 2100 and a selected area electron diffraction (SAED) pattern was taken for each sample. Images were obtained at 500, 200, 100, 50, 20, 10, 5, and 2 nm.[18]

RESULTS AND DISCUSSION

X-ray diffraction crystallography

Figure 1A shows the powder X-ray diffraction (XRD) patterns of MNP (Fe_3O_4), NHAP, MNHAP, and CPIC (24 h). The XRD pattern of MNP (Fe_3O_4) is closely similar to the standard JCPDS file for the Fe_3O_4 phase displaying peaks at 30.1°, 35.4°, 43.1°, 53.5°, 57°, and 62.6° representing the Miller planes (220), (311), (400), (422), (511), and (440) ascertained the presence of cubic unit structured Fe_3O_4 [Figure 1Aa]. The XRD pattern of the NHAP samples is shown in Figure 1Ab. The NHAP sample was confirmed by comparison of the obtained pattern with standard JCPDS files No. 09-0432 which showed the formation of hexagonal phase hydroxyapatite. The broad overlapped diffraction peaks observed in the range 30°–35° can be attributed to Miller planes (211), (112), (300), and (202) of HAP which revealed the formation of less crystalline hydroxyapatite nanoparticles. Indeed, NHAP coating over the MNP (Fe_3O_4) revealed the existence of both phases and it can be observed in Figure 1Ac. The presence of a diffraction peak corresponds to the (311) plane of magnetic phase in the MNHAP sample marked with the inverted triangle symbol. The XRD pattern of the prepared CPIC powder dried at 80ºC overnight revealed the amorphous phase which indicated the formation of amorphous calcium phosphate [Figure 1Ad].

Vibrating Sample Magnetometer (VSM) analysis for Fe_3O_4 and MNHAP

Room temperature *M(H)* plots of bare Fe_3O_4 (MNP) and

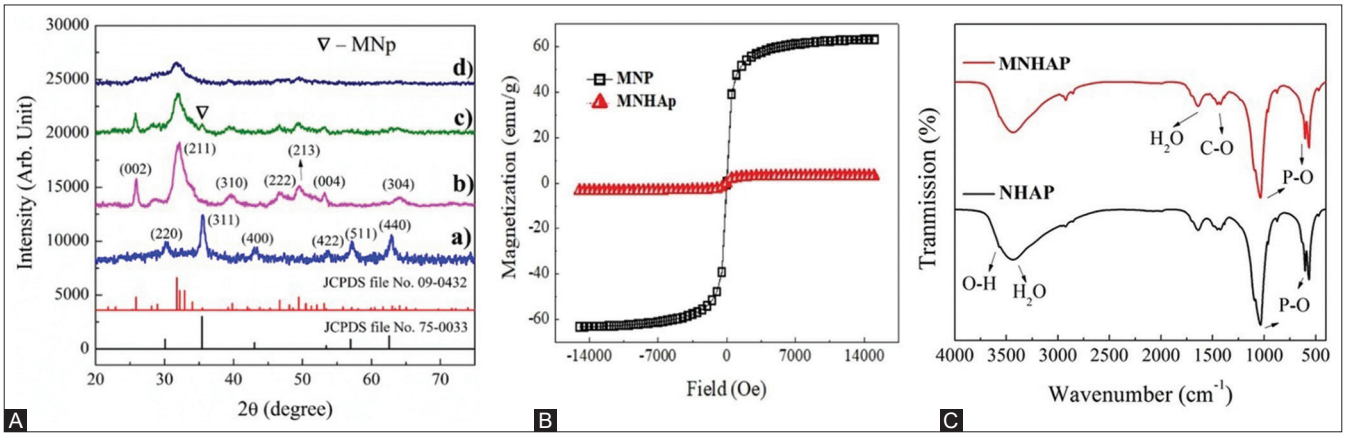

Figure 1: (A) (Powder XRD pattern of a) MNP (Fe_3O_4), b) NHAP, c) MNHAP, and d) CPIC samples). (B) M(H) plots of MNP (Fe_3O_4) and MNHAP samples. (C) Fourier transform infrared spectroscopy of NHAP and MNHAP samples

MNHAP samples were done with the applied field range of 15 kOe. The saturation magnetization was revealed to be 63.1 emu/g and 3.2 emu/g for Fe_3O_4 and MNHAP, respectively, with negligible coercivity at 8 Oe and 15 Oe. The shape of the plots with small coercivity displays the superparamagnetic behavior of the samples [Figure 1B]. The decrease of both saturation magnetization and coercivity in the MNHAP sample is due to the effect of nonmagnetic NHAP coating over the magnetic Fe_3O_4 phase, leading to affect interparticle interaction between the Fe_3O_4 particles. VSM analysis of synthesized Fe_3O_4 and MNHAP showed superparamagnetic behavior with small coercivity. The reduction in saturation magnetization and coercivity is owing to the coating of NHAP over magnetic nanoparticles (Fe_3O_4).

Cytotoxicity of MNHAP

Bare Fe_3O_4 magnetic nanoparticles were previously reported as biocompatible up to a 200 µg concentration.[19] MTT cytotoxicity assay using gingival fibroblast cells was used to test the biocompatibility of synthesized MNHAP. According to Biological Evaluation of Medical Devices-Part 5: tests for *in vitro* cytotoxicity (ISO 10993-5:2009), if the cell viability of the tested material is <70% then it has a cytotoxic capability.[20,21] From the data, synthesized MNHAP (magnetic nanoparticle encased with nanohydroxyapatite) was biocompatible at 50, 100, 200, 300, 400, and 500 µg concentrations at 24 h. This might be due to the nanohydroxyapatite coating over the Fe_3O_4 magnetic nanoparticles. At 48 h, more than 70% of cells are viable at 50, 100, and 200 µg, and the viability was reduced to below 70% at 300, 400, 500, and 600 µg concentrations [Figure 2 and Graph 1]. This might be due to the steady release of Fe^{3-} ions which may result in apoptosis of gingival fibroblast cells.

Fourier transform infrared spectroscopy

Characteristic P-O vibrations of hydroxyapatite were recorded at a wavenumber of 568, 606, and 1044 cm^{-1}. O-H stretching vibrations of hydroxyapatite were recorded at a wavenumber of 632 cm^{-1}. O-H stretching vibrations adhered to water molecules in both samples were recorded at 3410 and 1651 cm^{-1} wavenumber. Vibrational bands of carbonate ions were recorded at a wavenumber of 874 and 1428 cm^{-1}. The vibrational bands of Fe_3O_4 could not be distinguished from the MNHAP spectra which may be overlapped with the phosphate peaks of hydroxyapatite around 400–700 cm^{-1} [Figure 1C]. FTIR analysis of the synthesized MNHAP and Fe_3O_4 confirmed the presence of functional groups representing the Fe_3O_4 magnetic nanoparticles and nanohydroxyapatite.[22,23]

High-resolution transmission electron microscopy examination

NHAP

The shape of the hydroxyapatite crystals is elongated and rod-shaped. A substantial number of particles overlap to form agglomerates. The lack of homogenous distribution is due to the greater surface area of the hydroxyapatite crystals. The width of the crystal range between 5.08 and 11.92 nm. SAED pattern depicts the presence of a sharp and distinct continuous outer ring at 6.04 1/nm and an inner ring at 4.95 1/nm, substantiating the polycrystalline nature of the nanohydroxyapatite. The lattice fringes related to the (002) plane are 0.28 nm and 0.23 nm. The crystals are parallel to their longer axis (C-axis)[24] [Figure 3a-c].

MNHAP

The crystals were elongated and rod shaped. The particles agglomeration is due to their magnetic interaction. They are slightly larger than nanohydroxyapatite. The size of the crystals ranges from 13 nm to 29.47 nm. SAED showed the presence of a diffraction spot pattern at 5.49 1/nm. The lattice fringes correspond to the (002) plane is 0.26 nm[25] [Figure 3d-f].

Calcium and phosphate ion clusters + MNHAP

The crystals were polyhedral-in-shaped and were agglomerated. Crystal size is between 15.22 nm and 29.33 nm. In some areas, there are sheets of crystals due to the transition of spherical amorphous calcium phosphate to hydroxyapatite and its fusion with the MNHAP. SAED showed the continuous sharp distinct outer ring formed at 6.23 1/nm and a spotted inner ring formed at 4.21 1/

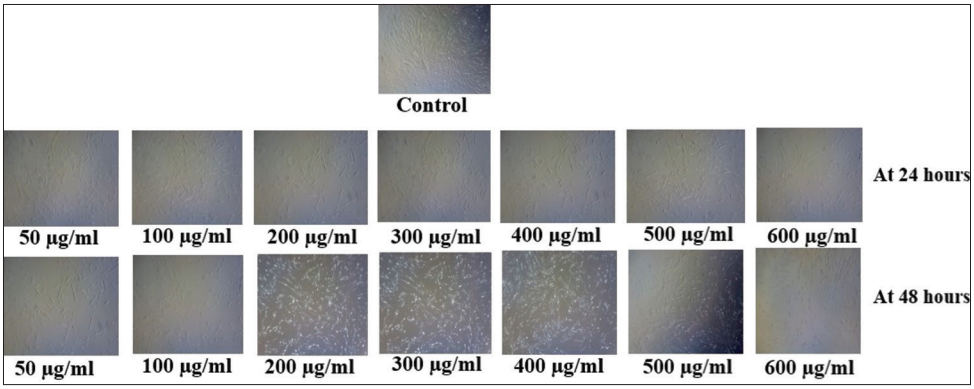

Figure 2: Showing the viability of gingival fibroblast cells at different concentrations

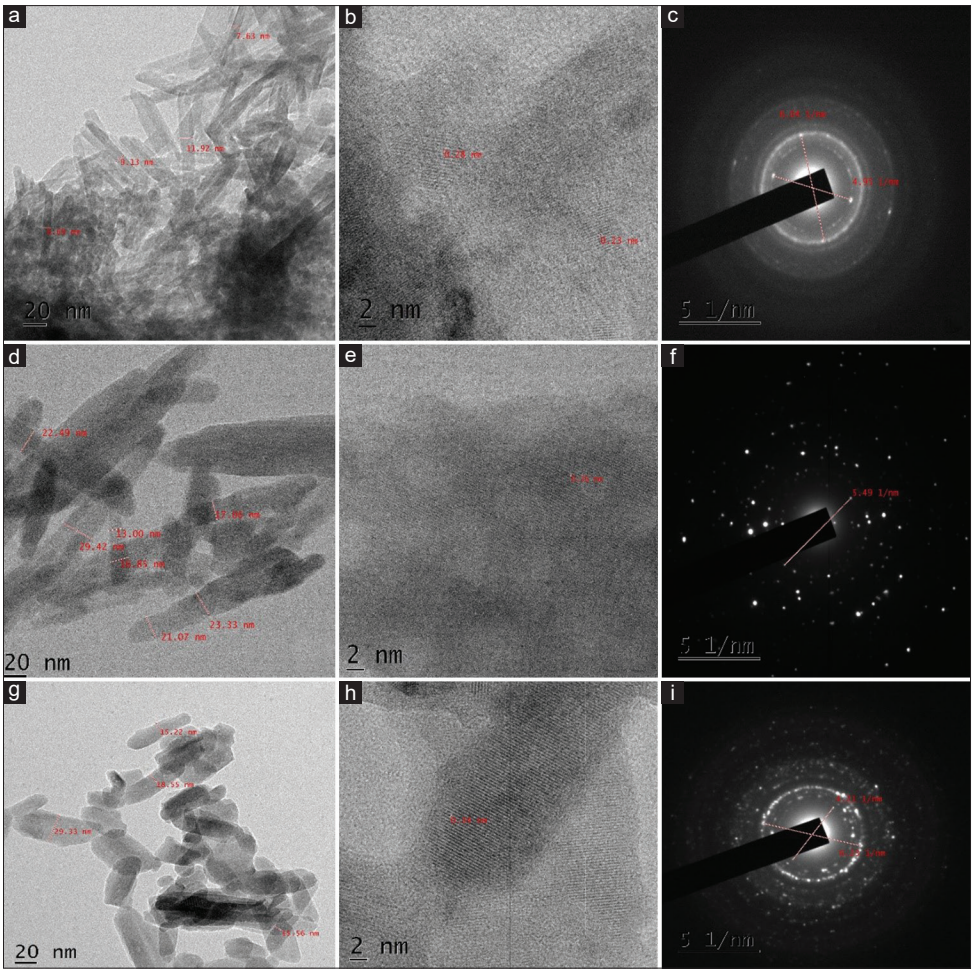

Figure 3: TEM images of NHAP (a-c), MNHAP (d-f), MNHAP + CPIC (g-i)

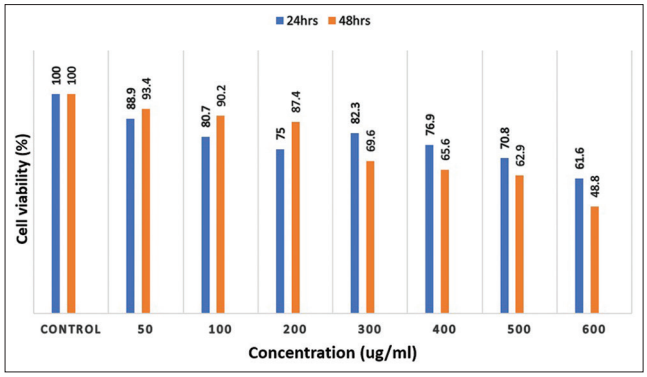

Graph 1: At 24 and 48 h, cell viability of MNHAP sample with gingival fibroblast cells

nm representing the polycrystalline nature. The lattice fringes are arranged parallel to the long axis at an interplanar distance of 0.34 nm corresponding to the (002) plane [Figure 3g-i].

Future studies exploring MNHAP and CPIC + MNHAP as remineralizing agents, in conjunction with magnetic field application, are warranted.

CONCLUSION

MNHAP was synthesized using wet precipitation, and CPICs were prepared using centrifugation. XRD confirms the presence of a magnetic phase at (311) peak in the MNHAP sample. Morphological analysis was performed using Transmission electron microscope (TEM), which showed the needle-shaped crystals in NHAP and MNHAP distinctly and the polyhedral arrangement of crystals in CPIC + MNHAP with a polycrystalline nature. Synthesized Fe_3O_4 and MNHAP exhibited superparamagnetic behavior. MTT assay at 48 h for MNHAP showed more than 70% survival at a concentration of 50, 100, and 200 µg, demonstrating potential cytocompatibility. MNHAP and a combination of CPIC + MNHAP might be pertinent as remineralizing agents for treating initial caries lesions with the application of a magnetic field.

Acknowledgments

We thank E. K. Girija and D. Karthickraja from the Department of Physics, Periyar University, Salem, for their support in synthesizing NHAP, MNHAP, CPIC, and conducting

XRD analysis. We also thank the Sophisticated Test and Instrumentation Centre for the TEM measurements.

This research was carried out as a part of the corresponding author' PhD thesis at DR. NTR UHS.

Financial support and sponsorship
Nil.

Conflicts of interest
There are no conflicts of interest.

REFERENCES

1. Bayda S, Adeel M, Tuccinardi T, Cordani M, Rizzolio F. The history of nanoscience and nanotechnology: From chemical-physical applications to nanomedicine. Molecules 2019;25:112.
2. Dvir T, Timko BP, Kohane DS, Langer R. Nanotechnological strategies for engineering complex tissues. Nat Nanotechnol 2011;6:13-22.
3. Zhang L, Webster TJ. Nanotechnology and nanomaterials: Promises for improved tissue regeneration. Nano Today 2009;4:66-80.
4. Baig N, Kammakakam I, Falath W. Nanomaterials: A review of synthesis methods, properties, recent progress, and challenges. Mater Adv 2021;2:1821-71.
5. Roduner E. Size matters: Why nanomaterials are different. Chem Soc Rev 2006;35:583-92.
6. Mehta AB, Kumari V, Jose R, Izadikhah V. Remineralization potential of bioactive glass and casein phosphopeptide-amorphous calcium phosphate on initial carious lesion: An *in-vitro* pH-cycling study. J Conserv Dent 2014;17:3-7.
7. Devadiga D, Shetty P, Hegde MN. Characterization of dynamic process of carious and erosive demineralization – An overview. J Conserv Dent 2022;25:454-62.
8. Sadat-Shojai M, Khorasani MT, Dinpanah-Khoshdargi E, Jamshidi A. Synthesis methods for nanosized hydroxyapatite with diverse structures. Acta Biomater 2013;9:7591-621.
9. Bandekar S, Patil S, Dudulwar D, Moogi PP, Ghosh S, Kshirsagar S. Remineralization potential of fluoride, amorphous calcium phosphate-casein phosphopeptide, and combination of hydroxylapatite and fluoride on enamel lesions: An *in vitro* comparative evaluation. J Conserv Dent 2019;22:305-9.
10. Rajendran R, Nair KR, Sandhya R, Ashik PM, Veedu RP, Saleem S. Evaluation of remineralization potential and cytotoxicity of a novel strontium-doped nanohydroxyapatite paste: An *in vitro* study. J Conserv Dent 2020;23:330-6.
11. Geeta RD, Vallabhaneni S, Fatima K. Comparative evaluation of remineralization potential of nanohydroxyapatite crystals, bioactive glass, casein phosphopeptide-amorphous calcium phosphate, and fluoride on initial enamel lesion (scanning electron microscope analysis) – An *in vitro* study. J Conserv Dent 2020;23:275-9.
12. Laurent S, Forge D, Port M, Roch A, Robic C, Vander Elst L, *et al.* Magnetic iron oxide nanoparticles: Synthesis, stabilization, vectorization, physicochemical characterizations, and biological applications. Chem Rev 2008;108:2064-110.
13. Li Y, Hu X, Xia Y, Ji Y, Ruan J, Weir MD, *et al.* Novel magnetic nanoparticle-containing adhesive with greater dentin bond strength and antibacterial and remineralizing capabilities. Dent Mater 2018;34:1310-22.
14. Shao C, Jin B, Mu Z, Lu H, Zhao Y, Wu Z, *et al.* Repair of tooth enamel by a biomimetic mineralization frontier ensuring epitaxial growth. Sci Adv 2019;5:eaaw9569.
15. Karunamoorthi R, Suresh Kumar G, Prasad AI, Vatsa RK, Thamizhavel A, Girija EK. Fabrication of a novel biocompatible magnetic biomaterial with hyperthermia potential. J Am Ceram Soc 2014;97:1115-22.
16. Karthi S, Govindan R, Gangadharan A, Dannangoda GC, Martirosyan KS, Sardar DK, *et al*. Luminomagnetic Nd3+ doped fluorapatite coated Fe3O4 nanostructures for biomedical applications. J Am Ceram Soc 2019;102:2558-68.
17. Leena M, Rana D, Webster TJ, Ramalingam M. Accelerated synthesis of biomimetic nano hydroxyapatite using simulated body fluid. Mater Chem Phys 2016;180:166-72.
18. Karthickraja D, Karthi S, Kumar GA, Sardar DK, Dannangoda GC, Martirosyan KS, *et al*. Fabrication of core–shell CoFe 2 O 4@ HAp nanoparticles: A novel magnetic platform for biomedical applications. New J Chem 2019;43:13584-93.
19. Karthi S, Kumar GA, Sardar DK, Dannangoda GC, Martirosyan KS, Girija EK. Fluorapatite coated iron oxide nanostructure for biomedical applications. Mater Chem Phys 2017;193:356-63.
20. Karthi S, Vivek P, Karthickraja D, Kumar GA, Dannangoda C, Martirosyan KS, *et al*. Synthesis of superparamagnetic zinc ferrite encased fluorapatite nanoparticles and its cytotoxicity effects on MG-63 cells. J Clust Sci 2022;1:1-7.
21. Kumar GS, Govindan R, Girija EK. *In situ* synthesis, characterization and *in vitro* studies of ciprofloxacin loaded hydroxyapatite nanoparticles for the treatment of osteomyelitis. J Mater Chem B 2014;2:5052-60.
22. Jadhav NV, Prasad AI, Kumar A, Mishra R, Dhara S, Babu KR, *et al.* Synthesis of oleic acid functionalized Fe3O4 magnetic nanoparticles and studying their interaction with tumor cells for potential hyperthermia applications. Colloids Surf B Biointerfaces 2013;108:158-68.
23. Fathi MH, Zahrani EM. Fabrication and characterization of fluoridated hydroxyapatite nanopowders via mechanical alloying. J Alloys Compd 2009;475:408-14.
24. Solla EL, Rodriguez-Gonzalez B, Pereiro I, Rodriguez-Valencia C, Cores BC, Serra J, *et al*. Nanonstructural analysis of hydroxyapatite thin films using HRTEM/FIB techniques. Microsc Microanal 2012;18:117-8.
25. Akhlaghinia B, Sanati P, Mohammadinezhad A, Zarei Z. The magnetic nanostructured natural hydroxyapatite (HAP/Fe3O4 NPs): An efficient, green and recyclable nanocatalyst for the synthesis of biscoumarin derivatives under solvent-free conditions. Res Chem Intermed 2019;45:3215-35.